

5							
11 6	CFAD_HUMAN	23	27016	5 (1)	4 (1)	0.14	Complement factor D OS=Homo sapiens GN=CFD PE=1 SV=5
11 7	MSTP9_HUMAN	23	79642	7 (1)	6 (1)	0.05	Putative macrophage-stimulating protein MSTP9 OS=Homo sapiens GN=MSTP9 PE=5 SV=2
11 8	PGCB_HUMAN	23	99056	8 (1)	8 (1)	0.04	Brevican core protein OS=Homo sapiens GN=BCAN PE=1 SV=2
11 9	GPR56_HUMAN	22	77688	4 (1)	4 (1)	0.05	G-protein coupled receptor 56 OS=Homo sapiens GN=GPR56 PE=1 SV=2
12 0	CELFR1_HUMAN	20	32927 8	22 (1)	22 (1)	0.01	Cadherin EGF LAG seven-pass G-type receptor 1 OS=Homo sapiens GN=CELSR1 PE=1 SV=1
12 1	ADML_HUMAN	18	20408	3 (1)	3 (1)	0.19	ADM OS=Homo sapiens GN=ADM PE=1 SV=1
12 2	CD99_HUMAN	17	18836	22 (1)	19 (1)	0.2	CD99 antigen OS=Homo sapiens GN=CD99 PE=1 SV=1
12 3	AEGP_HUMAN	17	13141 6	16 (1)	15 (1)	0.03	Apical endosomal glycoprotein OS=Homo sapiens GN=MAMDC4 PE=1 SV=2
12 4	GUC2A_HUMAN	17	12380	1 (1)	1 (1)	0.32	Guanylin OS=Homo sapiens GN=GUCA2A PE=1 SV=2

Table 4 糖尿病で微量アルブミン尿の患者の尿 (DN+)

Quantitation overview (112 proteins)							
		Score	Mass	Matches	Sequences	emPAI	
1	UROM_HUMAN	2442	69714	191 (132)	58 (35)	7.32	Uromodulin OS=Homo sapiens GN=UMOD PE=1 SV=1
2	ALBU_HUMAN	1137	69321	199 (79)	122 (51)	14.67	Serum albumin OS=Homo sapiens GN=ALB PE=1 SV=2
3	OSTP_HUMAN	651	35401	46 (28)	24 (14)	4.53	Osteopontin OS=Homo sapiens GN=SPP1 PE=1 SV=1
4	PCSK1_HUMAN	538	27356	22 (20)	11 (9)	2.21	ProSAAS OS=Homo sapiens GN=PCSK1N PE=1 SV=1
5	A1AT_HUMAN	520	46707	50 (27)	22 (10)	1.92	Alpha-1-antitrypsin OS=Homo sapiens GN=SERPINA1 PE=1 SV=3
6	FETUA_HUMAN	433	39300	36 (24)	27 (16)	3.69	Alpha-2-HS-glycoprotein OS=Homo sapiens GN=AHSG PE=1 SV=1
7	PIGR_HUMAN	419	83232	70 (30)	42 (18)	1.18	Polymeric immunoglobulin receptor OS=Homo sapiens GN=PIGR PE=1 SV=4
8	HBB_HUMAN	343	15988	26 (14)	17 (9)	7.76	Hemoglobin subunit beta OS=Homo sapiens GN=HBB PE=1 SV=2
9	GRN_HUMAN	329	63500	21 (9)	15 (4)	0.33	Granulins OS=Homo sapiens GN=GRN PE=1 SV=2
10	SAP_HUMAN	309	58074	24 (13)	13 (5)	0.86	Proactivator polypeptide OS=Homo sapiens GN=PSAP PE=1 SV=2
11	LTBP2_HUMAN	245	19493	6	18 (8)	0.14	Latent-transforming growth factor beta-binding protein 2 OS=Homo sapiens GN=LTBP2 PE=1 SV=2
12	FIBB_HUMAN	238	55892	14 (9)	8 (5)	0.38	Fibrinogen beta chain OS=Homo sapiens GN=FGB PE=1 SV=2
13	SLUR1_HUMAN	229	11178	20 (9)	7 (4)	3.55	Secreted Ly-6/uPAR-related protein 1 OS=Homo sapiens GN=SLURP1 PE=1 SV=2
14	AMBP_HUMAN	194	38974	16 (9)	9 (5)	0.58	Protein AMBP OS=Homo sapiens GN=AMBP PE=1 SV=1
15	CLUS_HUMAN	183	52461	14 (11)	8 (6)	0.51	Clusterin OS=Homo sapiens GN=CLU PE=1 SV=1
16	K2C1_HUMAN	178	65999	18 (6)	17 (5)	0.39	Keratin, type II cytoskeletal 1 OS=Homo sapiens GN=KRT1 PE=1 SV=6
17	VEGFA_HUMAN	178	27024	9 (6)	6 (4)	0.93	Vascular endothelial growth factor A OS=Homo sapiens GN=VEGFA PE=1 SV=2
18	PLMN_HUMAN	172	90510	13 (7)	11 (7)	0.32	Plasminogen OS=Homo sapiens GN=PLG PE=1 SV=2
19	UBIQ_HUMAN	160	8560	7 (6)	7 (6)	9.35	Ubiquitin OS=Homo sapiens GN=RPS27A PE=1 SV=1
20	K1C9_HUMAN	156	62027	14 (7)	14 (7)	0.42	Keratin, type I cytoskeletal 9 OS=Homo sapiens GN=KRT9 PE=1 SV=3
21	MASP2_HUMAN	153	75685	20 (10)	18 (9)	0.54	Mannan-binding lectin serine protease 2 OS=Homo sapiens GN=MASP2 PE=1 SV=3
22	TFF1_HUMAN	143	9143	8 (5)	6 (4)	5.29	Trefoil factor 1 OS=Homo sapiens GN=TFF1 PE=1 SV=1
23	TRFE_HUMAN	138	77000	18 (11)	15 (9)	0.52	Serotransferrin OS=Homo sapiens GN=TF PE=1 SV=2
24	APOA1_HUMAN	135	30759	13 (9)	11 (7)	1.52	Apolipoprotein A-I OS=Homo sapiens GN=APOA1 PE=1 SV=1
25.1	K2C6A_HUMAN	133	60008	11 (5)	10 (4)	0.35	Keratin, type II cytoskeletal 6A OS=Homo sapiens GN=KRT6A PE=1 SV=3
25.2	K2C6B_HUMAN	128	60030	11 (5)	10 (4)	0.35	Keratin, type II cytoskeletal 6B OS=Homo sapiens GN=KRT6B PE=1 SV=5
26	MSMB_HUMAN	130	12856	10 (5)	6 (2)	0.7	Beta-microseminoprotein OS=Homo sapiens GN=MSMB PE=1 SV=1
27	ISK1_HUMAN	126	8501	10 (7)	8 (7)	14.27	Pancreatic secretory trypsin inhibitor OS=Homo sapiens GN=SPINK1 PE=1 SV=2
28	PGRMC1_HUMAN	124	21658	8 (4)	6 (3)	0.63	Membrane-associated progesterone receptor component 1 OS=Homo sapiens GN=PGRMC1 PE=1 SV=3
29	ACTB_HUMAN	112	41710	15 (6)	11 (5)	0.53	Actin, cytoplasmic 1 OS=Homo sapiens GN=ACTB PE=1 SV=1
30	DEFB1_HUMAN	103	7415	5 (4)	4 (3)	2.76	Beta-defensin 1 OS=Homo sapiens GN=DEFB1 PE=1 SV=1
31	K2C5_HUMAN	101	62340	5 (3)	4 (3)	0.19	Keratin, type II cytoskeletal 5 OS=Homo sapiens GN=KRT5 PE=1 SV=3
32	SLUR2_HUMAN	100	10153	7 (4)	7 (4)	2.8	Secreted Ly-6/uPAR-related protein 2 OS=Homo sapiens GN=SLURP2 PE=2 SV=1
33	FN1_HUMAN	95	26244	2	13 (2)	0.03	Fibronectin OS=Homo sapiens GN=FN1 PE=1 SV=3
34	VGFB_HUMAN	94	67218	10 (5)	10 (5)	0.31	Neurosecretory protein VGF OS=Homo sapiens GN=VGFB PE=1 SV=2
35	THRB_HUMAN	93	69992	6 (2)	5 (1)	0.11	Prothrombin OS=Homo sapiens GN=F2 PE=1 SV=2
36	FBN1_HUMAN	90	31208	3	29 (4)	0.05	Fibrillin-1 OS=Homo sapiens GN=FBN1 PE=1 SV=2
37	K1C10_HUMAN	88	58792	2 (1)	2 (1)	0.06	Keratin, type I cytoskeletal 10 OS=Homo sapiens GN=KRT10 PE=1 SV=6
38	IGF2_HUMAN	86	20127	9 (5)	6 (3)	0.69	Insulin-like growth factor II OS=Homo sapiens GN=IGF2 PE=1 SV=1
39	THY1_HUMAN	85	17923	5 (3)	3 (1)	0.22	Thy-1 membrane glycoprotein OS=Homo sapiens GN=THY1 PE=1 SV=2
40	LAMC1_HUMAN	83	17748	9	15 (2)	0.04	Laminin subunit gamma-1 OS=Homo sapiens GN=LAMC1 PE=1 SV=3
41	ITIH2_HUMAN	79	10639	7	7 (2)	0.03	Inter-alpha-trypsin inhibitor heavy chain H2 OS=Homo sapiens GN=ITIH2 PE=1 SV=2
42	TFF2_HUMAN	78	14274	5 (2)	4 (1)	0.27	Trefoil factor 2 OS=Homo sapiens GN=TFF2 PE=1 SV=2
43	VTNC_HUMAN	77	54271	9 (3)	8 (2)	0.14	Vitronectin OS=Homo sapiens GN=VTN PE=1 SV=1
44	FIBA_HUMAN	76	94914	9 (2)	5 (2)	0.08	Fibrinogen alpha chain OS=Homo sapiens GN=FGA PE=1 SV=2
45	HBA_HUMAN	74	15248	6 (3)	6 (3)	0.98	Hemoglobin subunit alpha OS=Homo sapiens GN=HBA1 PE=1 SV=2
46	MGP_HUMAN	71	12345	15 (8)	8 (5)	3.01	Matrix Gla protein OS=Homo sapiens GN=MGP PE=1 SV=2
47	K1C16_HUMAN	70	51236	7 (2)	7 (2)	0.15	Keratin, type I cytoskeletal 16 OS=Homo sapiens GN=KRT16 PE=1 SV=4
48	A2AP_HUMAN	70	54531	6 (1)	6 (1)	0.07	Alpha-2-antiplasmin OS=Homo sapiens GN=SERPINF2 PE=1 SV=3
49	MT1G_HUMAN	56	6136	12 (3)	8 (3)	3.86	Metallothionein-1G OS=Homo sapiens GN=MT1G PE=1 SV=2
50	TTHY_HUMAN	69	15877	3 (1)	3 (1)	0.24	Transthyretin OS=Homo sapiens GN=TTR PE=1 SV=1
51	MA1A1_HUMAN	67	72922	4 (1)	4 (1)	0.05	Mannosyl-oligosaccharide 1,2-alpha-mannosidase IA OS=Homo sapiens GN=MAN1A1 PE=1 SV=3
52	COL1A1_HUMAN	67	17807	7	20 (5)	0.11	Collagen alpha-1(XVII) chain OS=Homo sapiens GN=COL1A1 PE=1 SV=5
53	TNFR12_HUMAN	64	13902	3 (2)	3 (2)	0.64	Tumor necrosis factor receptor superfamily member 12A OS=Homo sapiens GN=TNFRSF12A PE=1 SV=1
54	FBLN3_HUMAN	64	54604	3 (2)	2 (1)	0.07	EGF-containing fibulin-like extracellular matrix protein 1 OS=Homo sapiens GN=EFEMP1 PE=1 SV=2
55	IBP4_HUMAN	62	27915	4 (1)	4 (1)	0.14	Insulin-like growth factor-binding protein 4 OS=Homo sapiens GN=IGFBP4 PE=1 SV=2
56	HEPC3_HUMAN	60	9402	7 (4)	6 (3)	3.15	Hepcidin OS=Homo sapiens GN=HAMP PE=1 SV=2
57	CALL5_HUMAN	57	15883	2 (1)	2 (1)	0.24	Calmodulin-like protein 5 OS=Homo sapiens GN=CALL5 PE=1 SV=2
58	2B14_HUMAN	54	30093	4 (3)	2 (2)	0.27	HLA class II histocompatibility antigen, DRB1-4 beta chain OS=Homo sapiens GN=HLA-DRB1 PE=1 SV=1
59	BGAL_HUMAN	54	76027	4 (1)	4 (1)	0.05	Beta-galactosidase OS=Homo sapiens GN=GLB1 PE=1 SV=2
60	DNS2A_HUMAN	51	39556	1 (1)	1 (1)	0.09	Deoxyribonuclease-2-alpha OS=Homo sapiens GN=DNASE2 PE=1 SV=2
61	AT2B3_HUMAN	50	13411	2	9 (1)	0.03	Plasma membrane calcium-transporting ATPase 3 OS=Homo sapiens GN=ATP2B3 PE=1 SV=3
62	CDSN_HUMAN	50	51463	8 (2)	6 (1)	0.07	Corneodesmosin OS=Homo sapiens GN=CDSN PE=1 SV=2
63	EGF_HUMAN	50	13390	6	11 (2)	0.06	Pro-epidermal growth factor OS=Homo sapiens GN=EGF PE=1 SV=2
64	SAP3_HUMAN	50	20825	3 (1)	2 (1)	0.18	Ganglioside GM2 activator OS=Homo sapiens GN=GM2A PE=1 SV=4

65	NRAP_HUMAN	50	19695 0	4 (1)	4 (1)	0.02	Nebulin-related-anchoring protein OS=Homo sapiens GN=NRAP PE=2 SV=2
66	CD24_HUMAN	49	8092	1 (1)	1 (1)	0.51	Signal transducer CD24 OS=Homo sapiens GN=CD24 PE=1 SV=2
67	TNFR6_HUMAN	49	31464	3 (1)	3 (1)	0.12	Tumor necrosis factor ligand superfamily member 6 OS=Homo sapiens GN=TNFR6 PE=1 SV=1
68	ZAN_HUMAN	49	30537 4	24 (1)	20 (1)	0.01	Zonadhesin OS=Homo sapiens GN=ZAN PE=2 SV=3
69	TKNK_HUMAN	48	13430	1 (1)	1 (1)	0.29	Tachykinin-3 OS=Homo sapiens GN=TAC3 PE=1 SV=1
70	FBLN1_HUMAN	48	77162	9 (3)	9 (3)	0.15	Fibulin-1 OS=Homo sapiens GN=FBLN1 PE=1 SV=4
71	PK1L2_HUMAN	48	27237 1	15 (2)	9 (1)	0.01	Polycystic kidney disease protein 1-like 2 OS=Homo sapiens GN=PKD1L2 PE=1 SV=3
72	SHRM3_HUMAN	47	21652 8	8 (1)	8 (1)	0.02	Protein Shroom3 OS=Homo sapiens GN=SHROOM3 PE=1 SV=1
73	PENK_HUMAN	47	30767	4 (1)	4 (1)	0.12	Proenkephalin-A OS=Homo sapiens GN=PENK PE=1 SV=1
74	KLOT_HUMAN	47	11610 7	5 (3)	5 (3)	0.06	Klotho OS=Homo sapiens GN=KL PE=1 SV=2
75	WASL_HUMAN	47	54793	10 (1)	10 (1)	0.07	Neural Wiskott-Aldrich syndrome protein OS=Homo sapiens GN=WASL PE=1 SV=2
76	COT1A1_HUMAN	47	13882 7	11 (1)	10 (1)	0.03	Collagen alpha-1(I) chain OS=Homo sapiens GN=COL1A1 PE=1 SV=4
77	ATNG_HUMAN	44	7279	9 (2)	9 (2)	1.45	Sodium/potassium-transporting ATPase subunit gamma OS=Homo sapiens GN=FXD2 PE=1 SV=3
78	FBLN5_HUMAN	43	50147	7 (1)	7 (1)	0.07	Fibulin-5 OS=Homo sapiens GN=FBLN5 PE=1 SV=1
79	VTCN1_HUMAN	41	30859	1 (1)	1 (1)	0.12	V-set domain-containing T-cell activation inhibitor 1 OS=Homo sapiens GN=VTCN1 PE=1 SV=1
80	TSN9_HUMAN	41	26760	4 (1)	4 (1)	0.14	Tetraspanin-9 OS=Homo sapiens GN=TSPAN9 PE=1 SV=1
81	PIK3IP1_HUMAN	41	28230	2 (1)	2 (1)	0.13	Phosphoinositide-3-kinase-interacting protein 1 OS=Homo sapiens GN=PIK3IP1 PE=1 SV=2
82	2B1A_HUMAN	39	30055	3 (2)	2 (1)	0.13	HLA class II histocompatibility antigen, DRB1-10 beta chain OS=Homo sapiens GN=HLA-DRB1 PE=2 SV=1
83	2B1F_HUMAN	39	29947	5 (2)	3 (2)	0.27	HLA class II histocompatibility antigen, DRB1-15 beta chain OS=Homo sapiens GN=HLA-DRB1 PE=1 SV=2
84	APOA4_HUMAN	37	45371	7 (1)	5 (1)	0.08	Apolipoprotein A-IV OS=Homo sapiens GN=APOA4 PE=1 SV=3
85	SRGN_HUMAN	37	17641	1 (1)	1 (1)	0.22	Serglycin OS=Homo sapiens GN=SRGN PE=1 SV=3
86	TENX_HUMAN	37	46403 4	25 (1)	25 (1)	0.01	Tenascin-X OS=Homo sapiens GN=TNXB PE=1 SV=3
87	MEP1A_HUMAN	37	84365	7 (1)	7 (1)	0.04	Mepirin A subunit alpha OS=Homo sapiens GN=MEP1A PE=2 SV=2
88	DMBT1_HUMAN	37	26056 9	8 (1)	8 (1)	0.01	Deleted in malignant brain tumors 1 protein OS=Homo sapiens GN=DMBT1 PE=1 SV=2
89	TPP1_HUMAN	36	61210	5 (2)	4 (1)	0.12	Tripeptidyl-peptidase 1 OS=Homo sapiens GN=TPP1 PE=1 SV=2
90	SULF2_HUMAN	35	10039 0	6 (1)	5 (1)	0.04	Extracellular sulfatase Sulf-2 OS=Homo sapiens GN=SULF2 PE=1 SV=1
91	LMAN2_HUMAN	35	40203	6 (1)	4 (1)	0.09	Vesicular integral-membrane protein VIP36 OS=Homo sapiens GN=LMAN2 PE=1 SV=1
92	CO4A6_HUMAN	35	16370 4	25 (1)	24 (1)	0.02	Collagen alpha-6(IV) chain OS=Homo sapiens GN=COL4A6 PE=1 SV=3
93	IGHA2_HUMAN	35	36503	5 (1)	5 (1)	0.1	Ig alpha-2 chain C region OS=Homo sapiens GN=IGHA2 PE=1 SV=3
94	VTDB_HUMAN	34	52929	4 (1)	4 (1)	0.07	Vitamin D-binding protein OS=Homo sapiens GN=GC PE=1 SV=1
95	IGHG1_HUMAN	27	36083	16 (2)	10 (2)	0.22	Ig gamma-1 chain C region OS=Homo sapiens GN=IGHG1 PE=1 SV=1
96	CO3_HUMAN	33	18703 0	13 (1)	13 (1)	0.02	Complement C3 OS=Homo sapiens GN=C3 PE=1 SV=2
97	NIPBL_HUMAN	33	31585 4	14 (1)	14 (1)	0.01	Nipped-B-like protein OS=Homo sapiens GN=NIPBL PE=1 SV=2
98	CD99_HUMAN	32	18836	32 (2)	25 (2)	0.45	CD99 antigen OS=Homo sapiens GN=CD99 PE=1 SV=1
99	HPT_HUMAN	30	45177	4 (2)	4 (2)	0.17	Haptoglobin OS=Homo sapiens GN=HP PE=1 SV=1
100	TYB10_HUMAN	29	5023	1 (1)	1 (1)	0.87	Thymosin beta-10 OS=Homo sapiens GN=TMSB10 PE=1 SV=2
101	TETN_HUMAN	29	22552	4 (1)	4 (1)	0.17	Tetranectin OS=Homo sapiens GN=CLEC3B PE=1 SV=2
102	SHISA5_HUMAN	29	25564	7 (2)	6 (2)	0.32	Protein shisa-5 OS=Homo sapiens GN=SHISA5 PE=2 SV=1
103	CD59_HUMAN	28	14168	3 (1)	3 (1)	0.27	CD59 glycoprotein OS=Homo sapiens GN=CD59 PE=1 SV=1
104	TMSL1_HUMAN	27	5067	3 (2)	3 (2)	2.43	Thymosin beta-4-like protein 1 OS=Homo sapiens GN=TMSL1 PE=2 SV=1
105	ROBO4_HUMAN	26	10739 0	13 (1)	10 (1)	0.03	Roundabout homolog 4 OS=Homo sapiens GN=ROBO4 PE=1 SV=1
106	FURIN_HUMAN	26	86624	6 (1)	6 (1)	0.04	Furin OS=Homo sapiens GN=FURIN PE=1 SV=2
107	CATD_HUMAN	25	44524	7 (1)	6 (1)	0.08	Cathepsin D OS=Homo sapiens GN=CTSD PE=1 SV=1
108	UBP53_HUMAN	24	12073 0	4 (1)	4 (1)	0.03	Inactive ubiquitin carboxyl-terminal hydrolase 53 OS=Homo sapiens GN=USP53 PE=2 SV=2
109	ADML_HUMAN	24	20408	2 (1)	2 (1)	0.19	ADM OS=Homo sapiens GN=ADM PE=1 SV=1
110	FA78A_HUMAN	21	31947	2 (1)	2 (1)	0.12	Protein FAM78A OS=Homo sapiens GN=FAM78A PE=2 SV=1
111	HS3SA_HUMAN	20	44871	3 (1)	3 (1)	0.08	Heparan sulfate glucosamine 3-O-sulfotransferase 3A1 OS=Homo sapiens GN=HS3ST3A1 PE=1 SV=1

D. 考察

今回、糖尿病性腎症のバイオマーカー候補ペプチドを検出するために、臨床検体を用いて nanoLC/QSTAR システムを用いてペプチドのリスト化を行った。

今回のデータだけでも、各サンプル間において検出されたペプチドの種類に違いがあるため、バイオマーカー候補ペプチドになる可能性がある。

得られたペプチドは多数あり、MS/MS 解析の結果から、今後定量解析のための MRM 測定をする場合に必要な質量データも得ることができたため、測定したいターゲットを絞り込んだら、MRM 測定にて一斉に定量解析することができると思われる。

今後は、得られたバイオマーカー候補ペプチドと MS/MS データをもとに、MRM 測定し、多検体でのデータを収集して解析することで、糖尿病性腎症のバイオマーカーとなり得るペプチドを見いだ

したいと考えている。

E. 結論

糖尿病性腎症のバイオマーカー候補ペプチド探索の一步を踏み出したばかりであるが、今後さらにデータを集めることで、プロテオーム解析だけでは見つからなかったバイオマーカーが見つかることを期待している。

F. 健康危険情報

該当事項なし

G. 研究発表

論文：

学会発表：

該当事項なし

H. 知的財産権の出願・登録状況（予定を含む）

該当事項なし

Ⅲ. 研究成果の刊行に関する一覧表・別刷（平成20年度）

雑誌

発表者氏名	論文タイトル名	発表誌名	巻号	ページ	出版年
Yasuda K, Miyake K, Horikawa Y, Hara K, Oshawa H, Kasuga M, et al.	Variants in KCNQ1 are associated with susceptibility to type 2 diabetes mellitus.	Nat Gene	40	1092-1097	2009
Horikawa Y, Miyake K, Yasuda K, Enya M, Hirota Y, Kasuga M, et al.	Replication of genome-wide association studies of type 2 diabetes susceptibility in Japan.	J Clin Endocrinol Metab.	93	3136-3141	2008
Kaburagi Y, Yamashita R, Takahashi E, Yasuda K, Noda M.	Proteomic Studies on Investigations of Diabetes.	J Mass Spectrom Soc Jpn.			In press

研究成果の刊行に関する一覧表・別刷（平成21年度）

雑誌

発表者氏名	論文タイトル名	発表誌名	巻号	ページ	出版年
Y Okamoto K, Iwasaki N, Nishimura C, Doi K, Noiri E, Kasuga M, et al.	Identification of KCNJ15 as a susceptibility gene in Asian patients with type 2 diabetes mellitus	Am J Hum Genet.	86	54-64	2010
Miyake K, Yang W, Hara K, Yasuda K, Horikawa Y, Osawa H, Kasuga M, et al.	Construction of a prediction model for type 2 diabetes mellitus in the Japanese population based on 11 genes with strong evidence	J Hum Genet.	54	236-241	2009
Kaburagi Y, Yamashita R, Takahashi E, Yasuda K, Noda M.	Proteomic Studies on Investigations of Diabetes.	J Mass Spectrom Soc Jpn.	57	201-206	2009

研究成果の刊行に関する一覧表・別刷(平成22年度)

雑誌

発表者氏名	論文タイトル名	発表誌名	巻号	ページ	出版年
Takarabe D, Rokukawa Y, Takahashi Y, Goto A, Takaichi M, Okamoto M, Tsujimoto T, Notomi H, Kishimoto M, <u>Kaburagi Y</u> , Yasuda K, Yamamoto-Honda R, Tsukada K, Honda M, Teruya K, Kajio H, Kikuchi Y, Oka S, <u>Noda M.</u>	Autoimmune diabetes in HIV-infected patients on highly active antiretroviral therapy. J Clin Endocrinol Metab.	J Clin Endocrinol Metab.	95	4056-4060	2010
Tanaka T, Sakurada S, Kano K, Takahashi E, Yasuda K, Hirano H, <u>Kaburagi Y</u> , Kobayashi N, Le Hang NT, Lien LT, Matsushita I, Hijikata M, Uchida T, Keicho N.	Identification of tuberculosis-associated proteins in whole blood supernatant.	BMC Infect Dis.			In press
Unoki-Kubota H, Yamagishi S, Takeuchi M, Bujo H, Saito Y.	Pyridoxamine, an inhibitor of advanced glycation end product (AGE) formation ameliorates insulin resistance in obese, type 2 diabetic mice.	Protein Precept Lett.	17	1177-1181	2010

研究成果の刊行に関する一覧表・別刷(平成23年度)

雑誌

発表者氏名	論文タイトル名	発表誌名	巻号	ページ	出版年
Shim JH, Greenblatt M, B, Singh A, Brady N, Hu D, Drapp R, Ogawa W, <u>Kasuga m</u> , Noda T, Yang SH, Lee SK, Rebell VI, Glimcher LH.	Administration of BMP2/7 in utero partially reverses Rubinstein-Taybi syndrome-like skeletal defects induced by Pdk1 or Cbp mutations in mice.	J Clin Invest.	122	91-106	2012
Kimura K, Yamada T, Matsumoto M, Kido Y, Hosooka T, Asahara SI, Matsuda T, Ota T, Watanabe H, Sai Y, Miyamoto K, Kaneko S, <u>Kasuga m</u> , Inoue H.	Endoplasmic Reticulum Stress Inhibits STAT3-Dependent Suppression of Hepatic Gluconeogenesis via Dephosphorylation and Deacetylation.	Diabetes	61	61-73	2012
Tawaramoto K, Kotani K, Hashiramoto M, Kanda Y, Nagare T, Sakai H, Ogawa W, Emoto N, Yanagisawa M, Noda T, <u>Kasuga m</u> , Kaku K.	Ablation of 3-Phosphoinositide-Dependent Protein Kinase 1 (PDK1) in Vascular Endothelial Cells Enhances Insulin Sensitivity by Reducing Visceral Fat and Suppressing Angiogenesis.	Mol Endocrinol.	26	95-109	2012
Koyanagi M, Asahara S, Matsuda T, Hashimoto N, Shigeyama Y, Shibutani Y, Kanno A, Fujichita M, Mikami T, Hosooka T, Inoue H, Matsumoto M, Koike M, Uchiyama Y, Noda T, Seno S, <u>Kasuga m</u> , Kido Y.	Ablation of TSC2 enhances insulin secretion by increasing the number of mitochondria through activation of mTORC1.	PLoS One.	6	e23238	2011
Li S, Ogawa W, Emi A, Hayashi K, Senga Y, Nomura K, Hara K, Yuda D, <u>Kasuga m</u> .	Role of S6K1 in regulation of SREBP1c expression in the liver.	Biochem Biophys Res Commun.	412	197-202	2011

発表者氏名	論文タイトル名	発表誌名	巻号	ページ	出版年
Nagare T, Sakaue H, Matsumoto M, Cao Y, Inagaki K, Sakai M, Takashima Y, Nakamura K, Mori T, Okada Y, Matsuki Y, Watanabe E, Ikeda K, Taguchi R, Kamimura N, Ohta S, Hiramatsu R, <u>Kasuga m.</u>	Overexpression of KLF15 transcription factor in adipocytes of mice results in down-regulation of SCD1 protein expression in adipocytes and consequent enhancement of glucose-induced insulin secretion.	J Biol Chem.	286	37458-37469	2011
Cao Y, Nakata M, Okamoto S, Takano E, Yada T, Minokoshi Y, Hirata Y, Nakajima K, Iskandar K, Hayashi Y, Ongawa W, Barsh GS, Hosoda H, Kangawa K, Ito H, Noda T, <u>Kasuga m.</u> , Nakae J.	PDK1-Foxo1 in agouti-related peptide neurons regulates energy homeostasis by modulating food intake and energy expenditure.	PLoS One.	6	e18324	2011
Seike M, Saitou T, Kouchi Y, Ohara T, Matsuhisa M, Sakaguchi K, Tomita K, Kosugi K, Kashiwagi A, <u>Kasuga m.</u> , Tomita M, Naito Y, Nakajima H.	Computational assessment of insulin secretion and insulin sensitivity from 2-h oral glucose tolerance tests for clinical use for type 2 diabetes.	J Physiol Sci.	61	321-330	2011
Awazawa M, Ueki K, Inabe K, Yamauchi T, Kubota N, Kaneko K, Kobayashi M, Iwane A, Sasaki T, Okazaki Y, Ohnishi M, Takamoto I, Yamashita S, Asahara H, Akira S, <u>Kasuga m.</u> , Kadowaki T.	Adiponectin enhances insulin sensitivity by increasing hepatic IRS-2 expression via a macrophage-derived IL-6-dependent pathway.	Cell Metab.	13	401-412	2011

発表者氏名	論文タイトル名	発表誌名	巻号	ページ	出版年
Tsujimoto T, Kajio H, Takahashi Y, Kishimoto M, Noto H, Yamamoto-Honda R, Kamimura M, Morooka M, Kubota K, Shimbo T, Hiroe M, <u>Noda m.</u>	Asymptomatic coronary heart disease in patients with type 2 diabetes with vascular complications: a cross-sectional study.	BMJ Open.	1	e000139	2011
Ikeda N, Saito E, Konno N, Inoue M, Ikeda S, Satoh T, Wada K, Saito T, Katanoda K, Mizoue T, <u>Noda m.</u> , Iso H, Fujino Y, Sobue T, Tsugane S, Nagahashi M, Ezzati M, Shibuya K.	What has made the population of Japan healthy?	Lancet	378	1094-1105	2011
Nanri A, Mizoue T, <u>Noda m.</u> , Takahashi Y, Matsushita Y, Poudel-Tandukar K, Kato M, Obase S, Inoue M, Tsugane S; Japan Public Health Center-based Prospective Study Group.	Fish intake and type 2 diabetes in Japanese men and women: the Japan Public Health Center-based Prospective Study.	Am J Clin Nutr.	94	884-891	2011
Tanaka T, Morita A, Kato M, Hirai T, Mizoue T, Terauchi Y, Watanabe S, <u>Noda m.</u> ; SCOP Study Group.	Congener-specific polychlorinated biphenyls and the prevalence of diabetes in the Saku Control Obesity Program (SCOP).	Endocr J.	58	589-596	2011
Noto H, Tsujimoto T, Sasazuki T, <u>Noda m.</u>	Significantly increased risk of cancer in patients with diabetes mellitus: a systematic review and meta-analysis.	Endocr Pract.	17	616-628	2011

発表者氏名	論文タイトル名	発表誌名	巻号	ページ	出版年
Goto M, Yamamoto-Honda R, Shimbo T, Goto A, Terauchi Y, Kanazawa Y, <u>Noda m.</u>	Correlation between baseline serum 1,5-anhydroglucitol levels and 2-hour post-challenge glucose levels during oral glucose tolerance tests.	Endocr J.	58	13-17	2011
Hayashino Y, Suzuki H, Yamazaki K, Izumi K, <u>Noda m</u> , Kobayashi M.	Depressive symptoms, not completing a depression screening questionnaire, and risk of poor compliance with regular primary care visits in patients with type 2 diabetes: the Japan Diabetes Outcome Intervention Trial 2 (J-DOIT2) study group.	Exp Clin Endocrinol Diabetes.	119	276-280	2011
Nanri A, Mizoue T, Takahashi Y, Matsushita Y, <u>Noda m</u> , Inoue M, Tsugane S; Japan Public Health Center-based Prospective Study Group.	Association of weight change in different periods of adulthood with risk of type 2 diabetes in Japanese men and women: the Japan Public Health Center-Based Prospective Study.	J Epidemiol Community Health.	65	1104-1110	2011
Matsushita Y, Nakagawa T, Yamamoto S, Takahashi Y, <u>Noda m</u> , Mizoue T.	Associations of smoking cessation with visceral fat area and prevalence of metabolic syndrome in men: the Hitachi health study.	Obesity	19	647-651	2011

発表者氏名	論文タイトル名	発表誌名	巻号	ページ	出版年
Tanaka T, Sakurada S, Kano K, Takahashi E, Yasuda K, Hirano H, Kaburagi y, Kobayashi N, Le Hang NT, Lien LT, Matsushita I, Hij ikata M, Uchida T, Ke icho N.	Identification of tub erculosis-associated proteins in whole blo od supernatant.	BMC Infec t Dis.	11	71	2011
Kaburagi y, Unoki-Kub ota H.	Role of the podocyte signal-transduction s ystems in the pathoge nesis of diabetic nep hropathy.	Diabetol Int.	2	160-161	2011

研究成果の刊行に関する一覧表・別刷(平成24年度)

雑誌

発表者氏名	論文タイトル名	発表誌名	巻号	ページ	出版年
Takahashi E, Okumura A, Unoki-Kubota H, Hirano H, <u>Kasuga M</u> , <u>Kaburagi Y</u> .	Differential proteome analysis of serum proteins associated with the development of type 2 diabetes mellitus in the KK-A ^y mouse model using the iTRAQ technique.	J Proteomics.	84	40-51	2013
Kimura K, Nakamura Y, Inaba Y, Matsumoto M, Kido Y, Asahara SI, Matsuda T, Watanabe H, Maeda A, Inagaki F, Mukai C, Takeda K, Akira S, Ota T, Nakabayashi H, Kaneko S, <u>Kasuga M</u> , Inoue H.	Histidine augments the suppression of hepatic glucose production by central insulin action.	Diabetes.	印刷中		2013
Asahara S, Shibutani Y, Teruyama K, Inoue HY, Kawada Y, Etoh H, Matsuda T, Kimura-Koyanagi M, Hashimoto N, Sakahara M, Fujimoto W, Takahashi H, Ueda S, Hosooka T, Satoh T, Inoue H, Matsumoto M, Aiba A, <u>Kasuga M</u> , Kido Y.	Ras-related C3 botulinum toxin substrate 1 (RAC1) regulates glucose-stimulated insulin secretion via modulation of F-actin.	Diabetologia.	56	1088-97	2013
Takahashi M, Inomata S, Okimura Y, Iiguchi G, Fukuoka H, Miyake K, Koga D, Akamatsu S, <u>Kasuga M</u> , Takahashi Y.	Decreased serum chemerin levels in male Japanese patients with type 2 diabetes: sex dimorphism.	Endocr J.	60	37-44	2013
Kawano Y, Nakae J, Watanabe N, Fujisaka S, Iskandar K, Sekioka R, Hayashi Y, Tobe K, <u>Kasuga M</u> , Noda T, Yoshimura A, Onodera M, Itoh H.	Loss of Pdk1-Foxo1 signaling in myeloid cells predisposes to adipose tissue inflammation and insulin resistance.	Diabetes	61	1935-48	2012

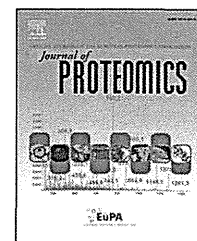
発表者氏名	論文タイトル名	発表誌名	巻号	ページ	出版年
Imamura M, Maeda S, Yamauchi T, Hara K, Yasuda K, Morizono T, Takahashi A, Horikoshi M, Nakamura M, Fujita H, Tsunoda T, Kubo M, Watada H, Maegawa H, Okada-Iwabu M, Iwabu M, Shojima N, Ohshige T, Omori S, Iwata M, Hirose H, Kaku K, Ito C, Tanaka Y, Toke K, Kashiwagi A, Kawamori R, <u>Kasuga M</u> , Kamatani N; Diabetes Genetics Replication and Meta-analysis (DIAGRAM) Consortium, Nakamura Y, Kadowaki T.	A single-nucleotide polymorphism in ANK1 is associated with susceptibility to type 2 diabetes in Japanese populations.	Hum Mol Genet.	21	3042-9	2012
Sakai M, Matsumoto M, Tujimura T, Yongheng C, Noguchi T, Inagaki K, Inoue H, Hosooka T, Takazawa K, Kido Y, Yasuda K, Hiramatsu R, Matsuki Y, <u>Kasuga M</u> .	CITED2 links hormonal signaling to PGC-1 α acetylation in the regulation of gluconeogenesis.	Nat Med.	18	612-7	2012
Hamasaki H, Yanai H, Mishima S, Mineyama T, Yamamoto-Honda R, Kakei M, Ezaki O, <u>Noda m</u> .	Correlations of non-exercise activity thermogenesis to metabolic parameters in Japanese patients with type 2 diabetes.	Diabetol Metab Syndr.	27	26	2013
Okamoto M, Kishimoto M, Takahashi Y, Osame K, Noto H, Yamamoto-Honda R, Kajio H, Tokuhara M, Edamoto Y, Endo H, Igari T, Kubota K, <u>Noda m</u> .	A case of malignant insulinoma: successful control of glycemic fluctuation by replacing octreotide injections with octreotide LAR injections.	Endocr J.	印刷中		2013
Kurotani K, Nanri A, Goto A, Mizoue T, <u>Noda m</u> , Oba S, Kato M, Matsushita Y, Inoue M, Tsugane S; for the Japan Public Health Center-based Prospective Study Group.	Red meat consumption is associated with the risk of type 2 diabetes in men but not in women: a Japan Public Health Center-based Prospective Study.	Br J Nutr.	7	1-9	2013

発表者氏名	論文タイトル名	発表誌名	巻号	ページ	出版年
Matsushita Y, Nakagawa T, Yamamoto S, Kato T, Ouchi T, Kikuchi N, Takahashi Y, Yokoyama T, Mizoue T, <u>Noda m.</u>	Adiponectin and visceral fat associated with cardiovascular risk factors.	Obesity	印刷中		2013
Goto M, Morita A, Goto A, Deura K, Sasaki S, Aiba N, Shimbo T, Terauchi Y, Miyachi M, <u>Noda m</u> , Watanabe S; SCOP Study Group.	Reduction in adiposity, β -cell function, insulin sensitivity, and cardiovascular risk factors: a prospective study among Japanese with obesity.	PLoS One.	8	e57964	2013
Matsushita Y, Nakagawa T, Yamamoto S, Takahashi Y, Yokoyama T, Mizoue T, <u>Noda m.</u>	Effect of longitudinal changes in visceral fat area on incidence of metabolic risk factors: The hitachi health study.	Obesity	印刷中		2013
Noto H, Goto A, Tsujimoto T, <u>Noda m.</u>	Low-carbohydrate diets and all-cause mortality: a systematic review and meta-analysis of observational studies.	PLoS One.	8	e55030	2013
Sakane N, Kotani K, Takahashi K, Sano Y, Tsuzaki K, Okazaki K, Sato J, Suzuki S, Morita S, Izumi K, Kato M, Ishizuka N, <u>Noda m</u> , Kuzuya H.	Japan Diabetes Outcome Intervention Trial-1 (J-DOIT1), a nationwide cluster randomized trial of type 2 diabetes prevention by telephone-delivered lifestyle support for high-risk subjects detected at health checkups: rationale, design, and recruitment.	BMC Public Health.	13	81	2013
Goto A, Morita A, Goto M, Sasaki S, Miyachi M, Aiba N, Terauchi Y, <u>Noda m</u> , Watanabe S; Saku Cohort Study Group.	Associations of sex hormone-binding globulin and testosterone with diabetes among men and women (the Saku Diabetes study): a case control study.	Cardiovasc Diabetol.	11	130	2012

発表者氏名	論文タイトル名	発表誌名	巻号	ページ	出版年
Kishimoto M, <u>Noda m.</u>	Effect of the addition of sitagliptin and miglitol on insulin-treated type 2 diabetes.	Diabetes Theor.	3	11	2012
Kishimoto M, <u>Noda m.</u>	The Great East Japan Earthquake: Experiences and Suggestions for Survivors with Diabetes (perspective).	PLoS Curr.	4	e:4facf9d99b997	2012
Goto M, Morita A, Goto A, Sasaki S, Aiba N, Shimbo T, Terauchi Y, Miyachi M, <u>Noda m.</u> , Watanabe S; SCOP Study Group.	Dietary glycemic index and glycemic load in relation to HbA1c in Japanese obese adults: a cross-sectional analysis of the Saku Control Obesity Program.	Nutr Metab	9	79	2012
Nanri A, Shimazu T, Takachi R, Ishihara J, Mizoue T, <u>Noda m.</u> , Inoue M, Tsubugane S; Japan Public Health Center-based Prospective Study Group.	Dietary patterns and type 2 diabetes in Japanese men and women: the Japan Public Health Center-based Prospective Study.	Eur J Clin Nutr	67	18-24	2013
Okumura A, Suzuki T, Miyatake H, Okabe T, Hashimoto Y, Miyakawa T, Zheng H, Unoki-Kubota H, Ohno H, Dohmae N, <u>Kaburagi y.</u> , Miyazaki Y, Tanokura	Leukocyte cell-derived chemotaxin 2 is a zinc-binding protein.	FEBS Let.	587	404-409	2013
Yokouchi H, Yasuda K, Takeda N, <u>Kaburagi y.</u> , Yamamoto S.	Angiopoietin-like protein 4 (ANGPTL4) is induced by high glucose in RPE cells and exhibits potent angiogenic activity on retinal endothelial cells.	Acta Ophthalmol	91	e289-297	2013

Available online at www.sciencedirect.com

SciVerse ScienceDirect

www.elsevier.com/locate/jprot

Differential proteome analysis of serum proteins associated with the development of type 2 diabetes mellitus in the KK-A^y mouse model using the iTRAQ technique

Eri Takahashi^{a,b,1}, Akinori Okumura^{a,1}, Hiroyuki Unoki-Kubota^{a,1}, Hisashi Hirano^b, Masato Kasuga^c, Yasushi Kaburagi^{a,*}

^aDepartment of Diabetic Complications, Diabetes Research Center, Research Institute, National Center for Global Health and Medicine, Tokyo, Japan

^bGraduate School of Nanobioscience, Yokohama City University, Yokohama, Japan

^cNational Center for Global Health and Medicine, Tokyo, Japan

ARTICLE INFO

Article history:

Received 24 October 2012

Accepted 19 March 2013

Keywords:

Serum proteome

Type 2 diabetes mellitus

Quantitative mass spectrometry

Multiple reaction monitoring

ABSTRACT

To identify candidate serum molecules associated with the progression of type 2 diabetes mellitus (T2DM), we carried out differential proteomic analysis using the KK-A^y mouse, an animal model of T2DM with obesity. We employed an iTRAQ-based quantitative proteomic approach to analyze the proteomic changes in the sera collected from a pair of 4-week-old KK-A^y versus C57BL/6 mice. Among the 227 proteins identified, a total of 45 proteins were differentially expressed in KK-A^y versus C57BL/6 mice. We comparatively analyzed a series of the sera collected at 4 and 12 weeks of age from KK-A^y and C57BL/6 mice for the target protein using multiple reaction monitoring analysis, and identified 8 differentially expressed proteins between the sera of these mice at both time points. Among them, serine (or cysteine) peptidase inhibitor, clade A, member 3K (SERPINA3K) levels were elevated significantly in the sera of KK-A^y mice compared to C57BL/6 mice. An *in vitro* assay revealed that the human homologue SERPINA3 increased the transendothelial permeability of retinal microvascular endothelial cells, which may be involved in the pathogenesis of diabetes and/or diabetic retinopathy. With the identified proteins, our proteomics study could provide valuable clues for a better understanding of the underlying mechanisms associated with T2DM.

Biological significance

In this paper, we investigated the serum proteome of KK-A^y mice in a pre-diabetic state compared to that of wild type controls in an attempt to uncover early diagnostic markers of diabetes that are maintained through a diabetic phenotype. We used iTRAQ-based two-dimensional LC-MS/MS serum profiling, and identified several differentially expressed proteins at the pre-diabetic stage. The differential expression was confirmed by multiple reaction monitoring assay, which is fast gaining ground as a sensitive, specific, and cost-effective methodology for relative quantification of the candidate proteins. Using these techniques, we have identified eight candidate proteins of interest including SERPINA3K, which may be important in the pathology of T2DM and/or diabetic retinopathy.

© 2013 Elsevier B.V. All rights reserved.

* Corresponding author at: Department of Diabetic Complications, Diabetes Research Center, Research Institute, National Center for Global Health and Medicine, 1-21-1 Toyama, Shinjuku-ku, Tokyo 162-8655, Japan. Tel.: +81 3 3202 7181x2931; fax: +81 3 3202 7364.

E-mail address: kaburagi@ri.ncgm.go.jp (Y. Kaburagi).

¹ Contributed equally.

1. Introduction

Diabetes mellitus is one of the most common metabolic disorders in the world, in which more than 90% of patients are diagnosed with type 2 diabetes mellitus (T2DM) [1]. The pathogenesis of T2DM is thought to be complicated, involving multiple genetic, metabolic, and environmental factors. Typically, it is characterized by hyperglycemia that is caused by defects in insulin secretion and its molecular action [2]. Initially, the effect of T2DM is limited to the detrimental loss of insulin-producing pancreatic β -cells. However, subsequent reduction in insulin secretion may lead to multiple malfunctions such as macrovascular complications including cardiovascular and cerebrovascular diseases, and microvascular complications including diabetic retinopathy and nephropathy [3].

Identifying individuals at high risk of T2DM prior to the clinical onset of the multiple malfunctions associated with T2DM is a major goal in diabetes research. Therefore, many efforts have been made to identify genetic and protein markers to reveal the molecular/cellular details or progression of diabetes [4–9]. Genome wide association studies have some clear advantages because genetic susceptibility, which does not change over time, can be identified at an early stage. While these markers provide a good foundation for the prediction and prevention of T2DM, the available tests are far from satisfactory due to their low-to-moderate sensitivity/specificity and/or late appearance in the disease process. As such, markers with increased specificity/sensitivity are urgently needed.

Proteomics has been used to identify novel disease markers that are differentially expressed during a pathological state in patients compared to healthy individuals. The systemic nature of T2DM indicates that the modulation of plasma proteins may be the cause or a consequence of the pathophysiology of this disease. To date, a few proteomic analyses of plasma related to T2DM have been reported [10–12]; however, analysis of the plasma proteomics of T2DM has been very limited and requires further investigations to find reliable diagnostic marker protein. Further, most previous serum proteomic analyses of T2DM have focused on the discovery of biomarkers, and have not stressed their potential to elucidate the pathophysiological mechanisms of the disease. Thus, the potential of serum proteomics to investigate the underlying disease mechanisms has been poorly addressed.

In this study, we analyzed the KK- A^y mouse model of T2DM in a pre-diabetic state. KK- A^y mice are obese, develop severe early-onset hyperinsulinemia, hyperglycemia, hypertriglyceridemia, and fatty liver, and are widely used as a model for T2DM [13]. We applied iTRAQ labeling coupled with offline 2-D LC-MS/MS proteomics technology to analyze quantitatively the protein expression profile of KK- A^y and C57BL/6 mice as well as to identify novel diagnostic marker proteins associated with the pathophysiological mechanisms of T2DM. To verify the candidate proteins that were differentially expressed among the two groups in the iTRAQ discovery study, we analyzed the time course changes of the candidate protein levels in the sera of KK- A^y and C57BL/6 mice using multiple reaction monitoring (MRM) analysis. We identified 8 proteins, including serine proteinase inhibitor A3K (SERPINA3K), that were expressed between the 2 groups. We further revealed that the human

homologue SERPINA3 increased the permeability of retinal microvascular endothelial cells, which may be involved in the pathogenesis of diabetes and/or diabetic retinopathy.

2. Materials and methods

2.1. Mouse sample collection

KK- A^y /TaJcl (KK- A^y) and C57BL/6Jcl (C57BL/6) mice were purchased from Clea Japan Inc. (Tokyo, Japan). The mice were housed individually and fed standard mouse chow and water. At 4, 8, 12 and 16 weeks of age, body weights and fasting blood glucose levels were measured as described previously ($n = 4$ /each group) [14]. Oral glucose tolerance test (OGTT) was performed on conscious mice after a 16 h fasting ($n = 4$ /each group). The test was done by orally administrated glucose (2 mg per g body weight) and measurement of blood glucose at 15, 30, 45 and 60 min after loading. To perform proteomic analysis associated with the early onset of T2DM, we studied 4- and 12-week-old KK- A^y and C57BL/6 mice as a reference. Blood samples were obtained from retro-orbital venous plexus of the mice which had fasted over 16 h. The serum was immediately separated by centrifugation at $3000 \times g$ for 20 min at 4 °C, and was stored at -80 °C until analyzed. Animal care, use, and experimental protocols were approved by the local animal ethics committee of the National Center for Global Health and Medicine (approval ID: 12034) and performed in accordance with EU Directive 2010/63/EU.

2.2. Protein depletion and purification

For each group (C57BL/6 mice at 4 weeks, KK- A^y mice at 4 weeks, C57BL/6 mice at 12 weeks, and KK- A^y mice at 12 weeks), serum samples were prepared from the male mice. The seven most abundant proteins (albumin, IgG, α 1-antitrypsin, IgM, transferrin, haptoglobin and fibrinogen) were depleted by using Seppro Mouse Spin Columns following the manufacturer's protocol (Sigma-Aldrich, St. Louis, MO, USA). The collected samples were desalted and concentrated using Amicon Ultra-4 3K (Millipore, Billerica, MA, USA). Protein concentration was determined using the Bradford protein assay (Bio-Rad Protein Assay; Bio-Rad Laboratories, Hercules, CA, USA).

2.3. iTRAQ labeling

An equal amount of depleted samples from each group was digested with MS-grade Trypsin Gold (Promega, Madison, WI, USA) and the peptides were labeled with iTRAQ reagents according to the manufacturer's instructions (iTRAQ Reagents 4-plex Applications Kit; AB Sciex, Framingham, MA, USA). Briefly, 25 μ g of each depleted sample was reduced with 50 mM tris-(2-carboxyethyl)phosphine, alkylated with 84 mM iodoacetamide, and digested with Trypsin Gold at a protein-to-enzyme ratio of 10:1 at 37 °C overnight. For the analysis of serum protein expression in the KK- A^y mice, the tryptic digest samples prepared from the 3 KK- A^y mice were labeled with iTRAQ reagents (iTRAQ reporter ions of 115.1, 116.1 and 117.1 m/z). An equal amount of samples from the 3 KK- A^y mice and 3 C57BL/6 mice was pooled, labeled with

iTRAQ reporter ions of 114.1 m/z , and used as an internal standard (Supplementary Fig. 1). The sample set consisting of the 3 KK-A^y mice samples and an internal standard were combined and dried using a centrifugal concentrator (TOMY SEIKO CO., LTD., Tokyo, Japan) and dissolved in 100 μL of 10 mM ammonium formate, 25% ACN and 0.5% formic acid. For the analysis of serum protein expression in the C57BL/6 mice, the tryptic digest samples prepared from the 3 C57BL/6 mice were labeled with iTRAQ reagents (iTRAQ reporter ions of 115.1, 116.1 and 117.1 m/z). The sample set consisting of the 3 C57BL/6 mice samples and an internal standard were combined, dried, and dissolved in 10 mM ammonium formate, 25% ACN and 0.5% formic acid as well.

2.4. Separation with strong cation exchange chromatography (SCX)

Two iTRAQ labeled sample sets were fractionated separately using HPLC (Gilson Medical, Middleton, WI, USA) equipped with a model 305 LC pump, a UV/VIS-155 detector, Rheodyne injection valve (model 7725) with 500 μL fixed loop injector, an FC203B autosampler, and a TSK gel SP-2SW column (4.6 mm I.D. \times 250 mm cm, ϕ 5 μm ; TOSOH, Tokyo, Japan) (Supplementary Fig. 1). The mobile phase consisted of (A); 10 mM ammonium formate and 25% ACN, pH 3.0 and (B); 500 mM ammonium formate and 25% ACN, pH 6.8. The mixed iTRAQ labeled samples were dissolved in 100 μL of buffer A and separated at a flow rate of 0.6 mL/min using a 2-step liner gradient; 0% B for 10 min, 0–30% B for 40 min, 30%–100% for 10 min, and 100% B for 10 min. A total of 18 fractions were collected, dried using the centrifugal concentrator, dissolved in 2% ACN and 0.1% TFA, and desalted with MonoSpin C18 (GL Science, Tokyo, Japan).

2.5. NanoLC–MS/MS

Fractionated samples prepared from each iTRAQ labeled sample set were analyzed by LC–MS/MS (Supplementary Fig. 1). NanoLC–MS/MS system was conducted by a QSTAR ELITE Q-TOF mass spectrometry (AB Sciex) equipped with a nano-electro-spray ionization source, a nanoLC system (Paradigm MS4; Michrom Bioresources, Auburn, CA, USA), and an HTC-PAL autosampler (CTC Analytics, Zwingen, Switzerland). The SCX-fractionated peptides dissolved in 2% ACN and 0.1% TFA were loaded onto a trap column (0.3 \times 5 mm, L-Column ODS; Chemicals Evaluation and Research Institute, Tokyo, Japan), and separated by RP capillary LC (L-Column Micro; Chemicals Evaluation and Research Institute) at a flow rate of 300 nL/min. The eluent gradient consisted of 95% buffer A (2% ACN and 0.1% TFA) to 45% buffer B (90% ACN and 0.1% TFA) for 120 min. A spray voltage of 1800 V was applied.

2.6. Data analysis of iTRAQ experiments

Peptide and protein identification was performed through automated database searching using the Mascot search engine (version 2.4.0; Matrix Science, London, UK). All tandem mass spectra were searched for species of *Mus musculus* against the UniProtKB/Swiss-Prot database containing 536,489 sequence entries (release—2012_06). Carbamidomethylation of cysteine

and iTRAQ reagents (N-terminus and Lysine side chain) were chosen as the fixed modifications, and oxidation of methionine and iTRAQ reagents (Tyrosine) were searched as the variable modifications. Searches were performed with trypsin cleavage specificity allowing 1 missed cleavage; mass tolerance for monoisotopic peptide identification was set to ± 0.1 Da and ± 0.1 Da for fragment ions. The instrument setting was “ESI-QUAD-TOF”. For the relative quantification of each peptide, the ratio of the areas under the signature peaks of 115, 116, 117, and 114 Da (as an internal standard), which are the masses of the tags that correspond to the iTRAQ reagents, was used. Data file processing and relative quantification were performed using ProteinPilot 3.0 software (AB Sciex) and the Paragon algorithm. The search parameters used were: iTRAQ 4-plex (peptide labeled), carbamidomethylation of cysteine, and UniProtKB/Swiss-Prot database for *M. musculus*. The confidence threshold for protein identification was an unused ProtScore > 1.3 (95% confidence interval). Protein quantification required at least one unique peptide, and relative protein quantitation value normalized to an internal standard for each sample was used for the statistical analysis.

2.7. Protein networks and functional analysis

Differentially expressed serum proteins between the KK-A^y and C57BL/6 mice were subjected to functional pathway analysis using Ingenuity Pathway Analysis (IPA) (Ingenuity Systems, available at www.ingenuity.com). Protein analysis was performed through Database for Annotation, Visualization and Integrated Discovery (DAVID) version 6.7 (available at <http://david.abcc.ncifcrf.gov/home.jsp>) [15].

2.8. Multiple reaction monitoring (MRM) analysis

For making transitions for each peptide in MRM, MRMPilot software version 2.0 (AB Sciex) was used. High-confidence peptides with a rich product ion spectrum for each target protein were selected for relative quantification analysis using MRM. Peptides that had modifications, such as partially oxidized methionine, were avoided and when possible, two peptides were used per protein. MRM run was performed using a 5500 QTRAP hybrid triple quadrupole/linear ion trap mass spectrometer (AB Sciex) coupled with a Paradigm MS4 nanoLC system in the MRM mode. Test runs of the synthetic peptides mixture were performed to establish the retention time window (± 5 min) for each peptide ion. During the test run, full scan MS/MS acquisitions (EPI, Enhanced Product Ion) were also triggered when MRM signal exceeded 1000 counts, with a mass tolerance of 250 mDa, the Linear Ion Trap (LIT) was set at 5 ms fixed fill time. Samples were separated on a C18 column (L-Column Micro, L-Column ODS; Chemicals Evaluation and Research Institute) with solvent A (2% ACN and 0.1% formic acid) and solvent B (90% ACN and 0.1% formic acid). The flow rate was set to 300 nL/min at room temperature, after which linear gradient elution was performed by increasing the mobile phase composition from 5 to 40% solvent B over 90 min. The gradient was then ramped to 95% B for 10 min and 5% B for 10 min to equilibrate the column for the next run. The total LC running time was 110 min. A 5500 QTRAP mass spectrometer was interfaced with a nanospray

source. The ionspray voltage was set to 2300 V. The source temperature was set to 150 °C. The curtain gas, collision gas, and ion source gas 1 were 10, 12, and 15, respectively. The declustering potential, entrance potential, and collision cell exit potential were set to 70 V, 10 V, and 15 V, respectively. Unit resolutions were used at quadrupole part 1 and quadrupole part 3. The collision energy for each transition was calculated by MRMPilot software version 2.0. In the MRM runs, the target scan time was set to 2 s. Five hundred ng of mouse serum sample was digested with mass spectrometry grade Trypsin Gold and Lysyl Endopeptidase (Wako Pure Chemicals, Osaka, Japan) for MRM analysis. The digested sample was transferred to a new tube and 10 fmol of human CUB domain containing protein 1 peptide (EEGVFTVTPDTK) was also added to each sample as an internal standard. Samples were analyzed by LC-MRM on the 5500 QTRAP using the predetermined MRM method. Data were processed using the MultiQuant program (version 2.0; AB Sciex). The most intense peak of the transition was used for quantitation. The area under the most intense peak was calculated, and normalized to the input internal standard. The peak of the transition for the input internal standard was also used for the quality control measure. Duplicate analyses were performed for each of the mouse serum samples.

2.9. Cell culture

Primary human retinal microvascular endothelial cells (HRMVECs) were purchased from the Applied Cell Biology Research Institute (Kirkland, WA, USA). HRMVECs were cultured on type I collagen-coated cell culture dishes in EGM-2 MV medium (EBM-2 supplemented with EGM-2 MV SingleQuots; Lonza, Walkersville, MD, USA). The cells were used at passages 7–9.

2.10. Expression and purification of recombinant human SERPINA3 protein

Human SERPINA3 cDNA excluding signal sequences was amplified from human liver mRNA (Clontech, Palo Alto, CA, USA) by RT-PCR and cloned into the expression vector pET-21a(+) (Merck KGaA, Darmstadt, Germany). The C-terminal histidine-tagged SERPINA3 protein was expressed in *Escherichia coli* BL21 (DE3) cells and purified by Ni-NTA affinity chromatography, as described previously [16]. The protein was passed through a polymyxin B affinity column (Detoxi-gel Endotoxin Removing Columns; Thermo Scientific, Rockford, IL, USA) to remove contaminating endotoxins. The eluted SERPINA3 protein was concentrated with a membrane filter (Amicon Ultra-15 3K; Millipore) and stored at –80 °C until use.

2.11. Electric cell substrate impedance sensing (ECIS) assays

Transendothelial electrical impedance was measured using an ECIS Z θ instrument (Applied Biophysics, Troy, NY, USA). HRMVECs were plated at confluence in 8W10E+ (for barrier functional measurement) or 8W1E (for wound-healing assay) gold electrode culture plates (Applied Biophysics) precoated with type I collagen. The cells were cultured in EGM-2 MV medium for 16 h, after which the medium was changed to

EBM-2 medium supplemented with 0.5% FBS (Lonza). For barrier functional measurement, HRMVECs were incubated with SERPINA3 protein at a final concentration ranging from 100 to 500 μ g/mL and the incubation was continued for a further 40 h. Multi-frequency measurements (11 frequencies at 0.0625, 0.125, 0.25, 0.5, 1, 2, 4, 8, 16, 32, and 64 kHz) were taken for each of the 16 wells at a fixed interval of 180 s. To better characterize the divergent changes in barrier function caused by SERPINA3 in HRMVECs, we applied the model of Giaever and Keese [17] to resolve our ECIS data into three components: Rb (cell-to-cell resistances), α (cell-to-extracellular matrix interaction), and Cm (membrane capacitance). For the wound-healing assays, serum-starved confluent cells treated with SERPINA3 at a final concentration ranging from 100 to 500 μ g/mL for 6 h were submitted to an elevated voltage pulse of 60 kHz frequency, 1400 μ A amplitude, and 20 s duration, which killed and removed cells from the electrode. The kinetics of wound closure over the electrode were then assessed by continuous impedance measurements at 16 kHz for 24 h. HRMVECs incubated without SERPINA3 were used as a control.

2.12. Cell proliferation analysis by 5-bromo-2'-deoxyuridine (BrdU) incorporation

HRMVECs (1.0×10^4 cells/well) were seeded in type I collagen-coated 96 well plates with EGM2 MV medium for 16 h and incubated with EBM2 medium supplemented with 0.5% FBS for another 8 h. The cells were treated with SERPINA3 protein for 18 h, after which BrdU labeling solution was added and incubated for another 6 h. The proliferation rate was measured using cell proliferation ELISA, BrdU chemiluminescence kit (Roche Applied Science, Mannheim, Germany) according to the manufacturer's protocol.

2.13. Data analysis and statistics

The distributions of continuous data were tested for normality by the Shapiro–Wilk test. Values were presented as mean \pm SD for normally distributed values. Differences between the groups were tested using Student's two-sided t-test or a two-tailed Mann–Whitney U test, as appropriate. All calculations were performed with Microsoft Excel 2010 or the SPSS software version 20 (IBM, Armonk, NY, USA). The differences were considered statistically significant for *p* values smaller than 0.05.

3. Results

3.1. Comparative analysis of the serum proteomic changes in the paired KK-A^y versus C57BL/6 mice

Characteristics of KK-A^y mice are shown in Fig. 1. KK-A^y mice were originally developed by Nishimura by crossing the KK mouse with the A^y mouse (C57BL/6J-A^y) [18]. C57BL/6J mice are generally used as nondiabetic controls. Therefore, we used C57BL/6J mice as a control for KK-A^y. As KK-A^y mice grew older, body weight and glucose concentration were gradually increased as reported previously [14]. Body weights of KK-A^y mice were significantly increased from 4 to 16 weeks of age